MNRAS **437,** 1208–1215 (2014)
Advance Access publication 2013 November 14
doi:10.1093/mnras/stt1924

Combined analysis of *Hubble* and VLT photometry of the intermediate mass black hole ESO 243−49 HLX-1

S. A. Farrell,[1⋆] M. Servillat,[2] J. C. Gladstone,[3] N. A. Webb,[4,5] R. Soria,[6] T. J. Maccarone,[7] K. Wiersema,[8] G. K. T. Hau,[9] J. Pforr,[10] P. J. Hakala,[11] C. Knigge,[12] D. Barret,[4,5] C. Maraston[13] and A. K. H. Kong[14]

[1]*Sydney Institute for Astronomy (SIfA), School of Physics, The University of Sydney, NSW 2006, Australia*
[2]*Laboratoire AIM, CEA Saclay, Bat. 709, F-91191 Gif-sur-Yvette, France*
[3]*Department of Physics, University of Alberta, Room 238 CEB, Edmonton, AB T6G 2G7, Canada*
[4]*Institut de Recherche en Astrophysique and Planétologie (IRAP), Université de Toulouse, UPS, 9 Avenue du colonel Roche, F-31028 Toulouse Cedex 4, France*
[5]*CNRS, UMR5277, F-31028 Toulouse, France*
[6]*International Centre for Radio Astronomy Research, Curtin University, GPO Box U1987, Perth, WA 6845, Australia*
[7]*Department of Physics, Texas Tech University, Box 41051, Lubbock, TX 79409-1051, USA*
[8]*Department of Physics and Astronomy, University of Leicester, University Road, Leicester LE1 7RH, UK*
[9]*European Southern Observatory, Alonso de Cordova 3107, Santiago, Chile*
[10]*NOAO, 950 North Cherry Ave., Tucson, AZ 85719, USA*
[11]*Finnish Centre for Astronomy with ESO (FINCA), Väisäläntie 20, University of Turku, FIN-21500 Piikkiö, Finland*
[12]*School of Physics and Astronomy, University of Southampton, Hampshire SO17 1BJ, UK*
[13]*Institute of Cosmology and Gravitation, University of Portsmouth, Dennis Sciama Building, Burnaby Road, Portsmouth PO1 3FX, UK*
[14]*Institute of Astronomy and Department of Physics, National Tsing Hua University, Hsinchu 30013, Taiwan*

Accepted 2013 October 7. Received 2013 October 7; in original form 2013 August 14

ABSTRACT

In this paper, we present a combined analysis of data obtained with the *Hubble Space Telescope* (*HST*), Very Large Telescope (VLT) and *Swift* X-ray telescope of the intermediate-mass black hole ESO 243−49 HLX-1 that were taken two months apart between 2010 September and November. Previous separate analyses of these data found that they were consistent with an irradiated accretion disc with contribution from either a very young or very old stellar population, and also indicated that the optical flux of the HLX-1 counterpart could be variable. Such variability could only be attributed to a varying accretion disc, so simultaneous analysis of all data sets should break the degeneracies in the model fits. We thus simultaneously fit the broad-band spectral energy distribution (SED) from near-infrared through to X-ray wavelengths of the two epochs of data with a model consisting of an irradiated accretion disc and a stellar population. We show that this combined analysis rules out an old stellar population, finding that the SED is dominated by emission from an accretion disc with moderate reprocessing in the outer disc around an intermediate-mass black hole imbedded in a young ($\sim$20 Myr) stellar cluster with a mass of $\sim 10^5$ $M_\odot$. We also place an upper limit on the mass of an additional hidden old stellar population of $\sim 10^6$ $M_\odot$. However, optical r'-band observations of HLX-1 obtained with the Gemini-South telescope covering part of the decay from a later X-ray outburst are consistent with constant optical flux, indicating that the observed variability between the *HST* and VLT observations could be spurious caused by differences in the background subtraction applied to the two optical data sets. In this scenario, the contribution of the stellar population, and thus the stellar mass of the cluster, may be higher. Nonetheless, variability of $<$50 per cent cannot be ruled out by the Gemini data and thus they are still consistent within the errors with an exponential decay similar to that observed in X-rays.

Key words: accretion, accretion discs – galaxies: dwarf – galaxies: interactions – X-rays: binaries – X-rays: individual: ESO 243−49 HLX-1.

⋆E-mail: sean.farrell@sydney.edu.au

1 INTRODUCTION

The formation of stellar-mass black holes ($\sim$3–80 $M_\odot$; Belczynski et al. 2010) through the collapse of massive stars is well accepted, but it is not yet completely clear how the supermassive black holes ($\sim10^6$–10^9 $M_\odot$) found in the centres of galaxies are formed. Two of the most promising theories are the stellar death and the direct collapse models (Volonteri 2010). Both scenarios predict that intermediate-mass black holes (IMBHs) with masses between $\sim10^{2-5}$ $M_\odot$ will have played an important role in the formation of supermassive black holes. The existence of IMBHs also has implications for other areas of astrophysics including for the modelling of hierarchical galaxy assembly (e.g. Hopkins et al. 2010), the search for dark matter annihilation signals (Fornasa & Bertone 2008), the epoch of reionization of the Universe (Ricotti & Ostriker 2004) and the detection of gravitational wave radiation (Abbott et al. 2009). The study of IMBHs and the environments in which they are found thus have important connotations for a wide range of important questions in modern astrophysics, and yet convincing evidence for their existence has until recently been scarce.

The brightest ultraluminous X-ray source ESO 243−49 HLX-1 (hereafter referred to simply as HLX-1) currently provides the strongest evidence for the existence of IMBHs (Farrell et al. 2009). HLX-1 is located in the halo of the edge-on S0a galaxy ESO 243−49, $\sim$0.8 kpc out of the plane and $\sim$3.3 kpc away from the nucleus in projection. At the redshift of ESO 243−49 ($z = 0.0223$) the maximum 0.2–10 keV X-ray luminosity of HLX-1 is $\sim10^{42}$ erg s^{-1} (Farrell et al. 2009), a factor of $\sim$400 above the theoretical Eddington limit for a 20 $M_\odot$ black hole. Luminosities up to $\sim10^{41}$ erg s^{-1} can be explained by stellar-mass black holes undergoing super-Eddington accretion (Begelman 2002) and/or experiencing significant beaming, which makes them appear to exceed the Eddington limit for isotropic radiation (Freeland et al. 2006; King 2008). However, luminosities above $\sim10^{41}$ erg s^{-1} are difficult to explain without a more massive black hole. Following the discovery of an optical counterpart by Soria et al. (2010), the distance to HLX-1 was confirmed through the detection of the Hα emission line at a redshift consistent with the scenario that HLX-1 is bound to ESO 243−49 (Wiersema et al. 2010), confirming the extreme luminosity. The redshift was recently corroborated through additional spectroscopic observations by Soria, Hau & Pakull (2013). Independent mass estimates obtained through Eddington scaling (Servillat et al. 2011), modelling the accretion disc emission (Davis et al. 2011; Godet et al. 2012a) and the detection of ballistic jets (Webb et al. 2012) imply a mass between $\sim$9000 and 90 000 $M_\odot$.

Long-term monitoring with the *Swift* X-ray telescope (XRT) has shown that HLX-1 varies in X-ray luminosity by a factor of $\sim$50 (Godet et al. 2009), with correlated spectral variability reminiscent of that seen in Galactic stellar-mass black holes (Servillat et al. 2011). Since the *Swift* monitoring began in 2009, HLX-1 has been observed to undergo four outbursts each spaced approximately one year apart (Godet et al. 2012a,b). The characteristic time-scales of the outbursts are inconsistent with the thermal-viscous instability model, and the outburst mechanism could instead be tidal stripping of a companion star in an eccentric orbit (Lasota et al. 2011). Lasota et al. (2011) concluded that in order to explain the implied high mass-loss rate of 10^{-4} $M_\odot$ yr^{-1} the donor star was most likely an asymptotic giant branch star with an initial mass of $\sim$0.5–10 $M_\odot$. Higher mass stars were disregarded based on the assumption that HLX-1 resided in a globular cluster with a minimum age of $\sim$0.3–0.6 Gyr. This scenario is supported by modelling of the outburst light curves under the assumption that the system is stable and the donor star will not be tidally disrupted within a few more cycles, and thus the donor star radius is not much larger than the instantaneous Roche lobe at periastron (Soria 2013).

Excess ultraviolet (UV) emission was detected at the position of HLX-1 with the *GALEX* UV space telescope and the *Swift* UV optical telescope, although this emission could not be resolved from the nucleus of ESO 243−49 (Webb et al. 2010). This UV excess is also consistent with the location of a pair of background galaxies at a redshift of $z \sim 0.03$, bringing into question the source of this emission (Wiersema et al. 2010; Farrell et al. 2011). In an attempt to uncover the nature of this UV excess, observations were obtained with the *Hubble Space Telescope* (*HST*) covering six filters from far-UV to near-IR bands following the peak of the second outburst on 2010 September 13 and 23. Farrell et al. (2012) analysed the broad-band spectral energy distribution (SED) using this *HST* data in combination with simultaneous *Swift* X-ray data, finding that while the X-ray spectrum was consistent with low temperature thermal emission from an irradiated accretion disc around an IMBH, the UV/optical/near-IR data were not. The addition of a component representing emission from a stellar cluster around the IMBH provided a statistically acceptable fit, but with two distinct solutions: a young ($\sim$13 Myr) stellar population with low level ($\ll$0.1 per cent) reprocessing in the outer disc, and an old ($\sim$13 Gyr) stellar population with extremely high ($\sim$10 per cent) reprocessing (both with stellar cluster masses of $\sim10^6$ $M_\odot$ and outer disc radii of $\sim$3000 times the inner disc radii). The level of reprocessing required in the old stellar population solution is borderline unphysically high, leading Farrell et al. (2012) to favour the young stellar population solution. In combination with the prominent dust lanes and lack of any nuclear activity in the host galaxy, the young stellar age and derived stellar mass suggests that HLX-1 may be the nuclear black hole remnant of a dwarf galaxy that was accreted and stripped by ESO 243−49 $<$ 200 Myr ago.

However, Very Large Telescope (VLT) optical photometric data covering the *UBVRI* bands obtained on 2010 November 7 and 26 by Soria et al. (2012) found that the optical flux had dropped by a factor of $\sim$2. Modelling the X-ray plus optical SED they found that it was entirely consistent with a pure irradiated disc model, and was not consistent with the presence of a massive (10^6 $M_\odot$) young stellar population. Soria et al. (2012) instead suggested that if some of the optical emission were associated with a stellar cluster, it was either a massive old population ($\sim10^6$ $M_\odot$, 10 Gyr) or a lower mass young population of stars ($\sim10^4$ $M_\odot$, $<$ 6 Myr). The questions of the age and mass of the stellar cluster in which HLX-1 is embedded and therefore the origin of the IMBH are thus still open.

In this paper, we report on the combined analysis of the *HST* data reported in Farrell et al. (2012) and the VLT data reported in Soria et al. (2012) along with the associated *Swift* X-ray data, fitting both data sets simultaneously with a combination of irradiated accretion disc and stellar population models. We also present an analysis of Gemini photometric monitoring data covering the third outburst of HLX-1 in an attempt to provide independent confirmation of the optical variability.

2 DATA REDUCTION AND ANALYSIS

2.1 *HST*, VLT and *Swift* data

For the analyses described below, we use the same reduced data (obtained with the *HST*, VLT and *Swift* telescopes) presented in Farrell et al. (2012) and Soria et al. (2012). Both sets of *Swift* spectra were binned to a minimum of 20 counts per bin in order to

use χ^2 statistics for the fitting. The VLT magnitudes were converted into XSPEC-readable spectral files using the same method outlined in Farrell et al. (2012). For the SED fitting, we utilized the XSPEC v12.6.0q software (Arnaud 1996).

We first fitted the *Swift* (hereafter referred to as S2) and VLT data used in Soria et al. (2012) with the irradiated disc model (*diskir*; Gierliński, Done & Page 2008, 2009), with multiplicative components representing absorption by the neutral hydrogen column $N_{\rm H}$ (using the *tbabs* model and the elemental abundances prescribed in Lodders 2003) and dust extinction $E(B-V)$ (using the *redden* model and the extinction curves in Cardelli, Clayton & Mathis 1989) included. The absorption and extinction values were constrained to be greater than or equal to the Galactic values in the direction of HLX-1, i.e. 1.79×10^{20} atoms cm^{-2} (Kalberla et al. 2005) and 0.013 mag (Schlegel, Finkbeiner & Davis 1998), respectively. This is the same model that Soria et al. (2012) utilized; however, they did not fit the S2 and VLT data simultaneously in XSPEC.

We initially froze the high-energy turn over (kT_e), Compton inner disc fraction ($f_{\rm in}$), radius of the Compton-illuminated disc ($r_{\rm irr}$), fraction of flux thermalized in the outer disc ($f_{\rm out}$) and the ratio of the outer disc to inner disc radii ($\log(r_{\rm out}/r_{\rm in})$) parameters at the same values as assumed by Soria et al. (2012). The other parameters including the inner disc temperature ($kT_{\rm disc}$), the photon index of the Compton tail (Γ), the ratio of Compton to disc luminosities ($L_{\rm c}/L_{\rm d}$) and the model normalization ($N_{\rm disc}$) were all allowed to vary freely. We obtained an acceptable fit with this model with $\chi^2_\nu = 0.87$ for 57 degrees of freedom and model parameters all consistent within the errors with those reported in Soria et al. (2012). We next thawed the $f_{\rm out}$ and $\log(r_{\rm out}/r_{\rm in})$ values and refitted the SED, as by fitting the VLT+S1 data simultaneously we should be able to place some constraints on the properties of the outer disc. We obtained a good fit with this model with the parameters reported in Table 1.

Table 1. Best-fitting parameters for the independent fitting of the *HST*+S1 and VLT+S2 data with the irradiated disc model. For the *HST* data, the far-UV data point was excluded. A description of each of the parameters is given in the text. The parameter values in brackets were frozen at the values indicated. The disc luminosities ($L_{0.2-10\,\rm keV}$) are over the energy range of 0.2–10 keV (and are unabsorbed and dereddened). Errors are at the 90 per cent confidence level.

Parameter	*HST*+S1	VLT+S2	Units
$E(B-V)^a$	$0.013^{+0.05}_{-0.01}$	$0.013^{+0.50}_{-0.01}$	mag
$N_{\rm H}$	$0.15^{+0.07}_{-0.09}$	$0.03^{+0.03}_{-0.03}$	10^{22} cm^{-2} s^{-1}
$kT_{\rm disc}$	$0.17^{+0.03}_{-0.02}$	$0.17^{+0.02}_{-0.05}$	keV
Γ	[2.1]	$1.7^{+0.7}_{-0.4}$	
kT_e	[100]	[100]	keV
$L_{\rm c}/L_{\rm d}$	$0.07^{+0.06}_{-0.03}$	$0.4^{+4.0}_{-0.3}$	
$f_{\rm in}$	[0.0]	[0.1]	
$r_{\rm irr}$	[1.0001]	[1.2]	$r_{\rm in}$
$f^b_{\rm out}$	$0.0013^{+0.0030}_{-0.0008}$	$0.0025^{+0.100}_{-0.002}$	
$\log(r_{\rm out}/r_{\rm in})$	$3.7^{+0.1}_{-0.2}$	$3.5^{+0.5}_{-4.0}$	
$N_{\rm disc}$	100^{+200}_{-100}	40^{+30}_{-10}	
$L_{0.2-10\,\rm keV}$	1.9×10^{42}	0.7×10^{42}	erg s^{-1}
χ^2/d.o.f.	26.0/29	48.5/55	

[a]The extinction pegged at the Galactic value of 0.013 mag for both sets of data.

[b]The fraction of flux thermalized in the outer disc pegged at the hard upper limit of the model for the VLT+S2 data.

As reported in Farrell et al. (2012), fitting of the *HST* and simultaneous *Swift* (hereafter referred to as S1) data found that the SED was not consistent with a pure disc model ($\chi^2_\nu = 1.6$ for 30 degrees of freedom), with a clear excess detected in the far-UV that was modelled by Farrell et al. (2012) using a stellar population component. By removing the far-UV data point from our SED fitting, we can obtain a good fit with the pure irradiated disc model (see Table 1 for the best-fitting model parameters). However, the UV excess indicates that additional components are required to account for the SED. So, although the VLT+S2 data on their own do not explicitly require a more complicated model, an additional model component representing emission from a stellar cluster is required in order to describe the *HST*+S1 data.

The emission from the accretion disc around HLX-1 is known to vary in flux considerably over time (Servillat et al. 2011). In contrast, the emission from a stellar cluster should be stable, allowing us to use the variability of the disc to break the degeneracies in the model fitting encountered by Farrell et al. (2012). We therefore fitted the *HST*+S1 and VLT+S2 data simultaneously using the *diskir* model with the addition of the same Maraston (2005) theoretical stellar population model[1] used by Farrell et al. (2012). For the simultaneous fitting, we allowed the disc parameters to vary freely between the two sets of data, using the same constraints on the *diskir* parameters as used by Farrell et al. (2012) and Soria et al. (2012), but tied the stellar population parameters together. However, unlike in Soria et al. (2012) we did not freeze the fraction of flux from the inner disc that is reprocessed in the outer disc (i.e. the $f_{\rm out}$ parameter) for the irradiated disc model fitted to the VLT+S2 data. We first attempted tying the $f_{\rm out}$ parameter between the two epochs of data, but found that the model tended to overpredict the disc emission in the VLT bands. This could possibly imply that the disc geometry (i.e. the disc height, solid angle, etc.) and/or the albedo varied between the observations. We thus decided to allow $f_{\rm out}$ to vary freely. We also kept the outer disc radius parameter $\log(r_{\rm out}/r_{\rm in})$ tied between the two data sets, as the luminosity of the thermal component has been seen to vary as $L_{\rm d} \sim T_{\rm in}^4$ (Servillat et al. 2011, consistent with emission from the inner part of an accretion disc) and the X-ray decline between the two epochs is exponential, which is expected once supply to the disc ceases if the outer disc radius is constant (King & Ritter 1998). Absorption and extinction were accounted for as described above, with the parameters tied between the two data sets.[2]

We obtained an excellent fit with the irradiated disc plus the Maraston (2005) stellar population model, with the best fit providing physically plausible parameter values (see Table 2). The best-fitting SED models are shown in Fig. 1. It should be noted that there is a large disparity between the size of the error bars in the *HST* and VLT data, so the *HST* data dominate the fit. In addition, the largest contribution from the stellar population model is in the UV bands, which are not sampled by the VLT data, thus introducing the far-UV *HST* data point has a disproportionate influence on the model fitting. As noted above, without the *HST* far-UV data point both SEDs are consistent with a pure irradiated accretion disc model,

[1] http://www.maraston.eu/Xspec_models

[2] We should note that we experimented with allowing the $N_{\rm H}$ to vary freely but found that while the degrees of freedom were reduced the model fitting was not improved. As such, we chose to link the parameters between the two data sets under the assumption that the $N_{\rm H}$ likely does not vary significantly over the time-scale between the two sets of observations.

Table 2. Best-fitting parameters for the simultaneous fitting of the *HST*, VLT and *Swift* data with the irradiated disc plus stellar population models, with the disc component allowed to vary freely but the stellar population fixed between the two epochs of data. A description of each of the parameters is given in the text. The parameters values in brackets were frozen at the values indicated. The luminosity for the stellar population is bolometric, while the disc luminosities ($L_{0.2-10\,\mathrm{keV}}$) are over the energy range of 0.2–10 keV (all luminosities are unabsorbed and dereddened). The luminosity and thus the mass of the stellar population component are highly unconstrained, thus we quote only the best-fitting value here. Errors are at the 90 per cent confidence level.

Parameter	*HST*+S1	VLT+S2	Units
	Extinction and absorption		
$E(B-V)^a$	$0.013^{+0.12}_{-0.00}$		mag
$N_{\rm H}$	$0.04^{+0.03}_{-0.02}$		10^{22} cm^{-2} s^{-1}
	Stellar population		
Z_*	[1.0]		$Z_\odot$
Age	2^{+6}_{-2}		10^7 yr
z	[0.0223]		
L_*	$\sim 2 \times 10^{40}$		erg s^{-1}
M_*	$\sim 9 \times 10^4$		$M_\odot$
	Irradiated accretion disc		
$kT_{\rm disc}$	0.20±0.02	$0.17^{+0.01}_{-0.02}$	keV
Γ	[2.1]	$1.8^{+0.7}_{-0.5}$	
kT_e	[100]	[100]	keV
$L_{\rm c}/L_{\rm d}$	$0.11^{+0.08}_{-0.07}$	$0.3^{+2.0}_{-0.2}$	
$f_{\rm in}$	[0.0]	[0.1]	
$r_{\rm irr}$	[1.0001]	[1.2]	$r_{\rm in}$
$f_{\rm out}$	$3.7^{+0.3}_{-2.0}$	$0.8^{+0.3}_{-0.8}$	10^{-3}
$\log(r_{\rm out}/r_{\rm in})$	$4.0^{+0.4}_{-0.2}$		
$N_{\rm disc}$	30^{+20}_{-10}	50^{+50}_{-20}	
$L_{0.2-10\,\mathrm{keV}}$	1×10^{42}	0.8×10^{42}	erg s^{-1}
χ^2/d.o.f.	73.79/86		

[a]The extinction pegged at the Galactic value of 0.013 mag.

highlighting the importance of UV data in order to correctly model the broad-band SED.

The metallicity (Z_*) of the stellar population could not be constrained and so we froze it to solar values (the metallicity of ESO 243−49 has not previously been measured, so we chose $Z_* = 1\,Z_\odot$ as it is the approximate mid-point of the metallicity range in the Maraston 2005, model). The best-fitting age of the stellar population was found to be ∼20 Myr, with the luminosity (L_*) and thus stellar mass (M_*) lower than that found from fitting the *HST*+S1 data alone. Changing the metallicity to $Z_* = 0.2$ or $2.0\,Z_\odot$ does not change the other parameters of the fit significantly, indicating that the fit is completely insensitive to metallicity. The stellar mass of the best combined fit (calculated using the assumed metallicity, the derived age and bolometric luminosity, and the model mass-to-light ratio[3]) was found to be $9 \times 10^4\,M_\odot$, more than an order of magnitude lower than reported by Farrell et al. (2012). It should be noted, however, that the large uncertainties in the luminosity (in part due to the large errors in the absorption and extinction), age and metallicity of the stellar population produce very large errors in the stellar mass. Taking into account the errors on luminosity and age, and the allowable ranges of metallicity in the stellar population model (i.e. $Z_* = 0.2$–$2.0\,Z_\odot$), we very roughly constrain the mass to be between $\sim 5 \times 10^2$ and $6 \times 10^6\,M_\odot$.

In contrast to the results of fitting the *HST*+S1 alone, by fitting the *HST*+S1 and VLT+S2 data simultaneously we found that the old stellar population solution is no longer viable. The χ^2 contour plots of the stellar population age against $f_{\rm out}$ are presented in Figs 2 and 3, showing that while an old (>1 Gyr) stellar population is viable when only considering the *HST*+S1 data alone, when fitting the *HST*+S1 and the VLT+S2 data simultaneously the old stellar population solution is no longer acceptable. The reason for this is that significant variability is observed between the red end of the *HST* and VLT data, which by definition requires the disc to make a significant/dominant contribution at that end of the SED, thus ruling out the possibility of an old population (which would only be able to contribute at that end of the SED). These results thus support the conclusions of Farrell et al. (2012) but with a lower stellar mass (as suggested by Soria et al. 2012).

The stellar population model component, however, only accounts for the dominant stellar population. Our results thus imply that there was a recent burst of star formation in the cluster ∼20 Myr ago, and while older stars are almost certainly also present young stars currently dominate the stellar light. Although the statistics of our data are insufficient to allow us to attempt to fit for an additional old stellar contribution, we attempted to place limits on the luminosity and thus mass of the underlying old population. Taking our best-fitting solution to the SED, we added an additional stellar population model with the metallicity frozen at $1.0\,Z_\odot$, the stellar age frozen at 10 Gyr, and the redshift frozen at 0.0223, and steadily increased the normalization of this component until we could no longer obtain an acceptable fit at the 90 per cent confidence level. In this manner, we found that the upper limit on the bolometric luminosity (unabsorbed and deredenned) of the old stellar population was $\sim 10^{39}$ erg s^{-1}, giving a mass upper limit of $\sim 10^6\,M_\odot$. Thus, while the light from the stellar cluster appears to be dominated by a young population of stars, the data do not exclude a lower luminosity population of older stars dominating the mass of the cluster.

The irradiated disc models fitted to both the *HST*+S1 and VLT+S2 data (for the best-fitting disc plus young stellar population solution) had physically plausible parameters broadly consistent with those reported previously by Farrell et al. (2012) and Soria et al. (2012). The accretion disc temperatures agree within the errors with those reported by Farrell et al. (2012) and Soria et al. (2012), as well as the $L_{\rm disc} \propto T_{\rm in}^4$ trend reported by Servillat et al. (2011) and expected for a geometrically thin, optically thick accretion disc (Shakura & Sunyaev 1973). The disc luminosities were also very similar to those reported previously, as were the ratios of Compton tail to disc luminosities ($L_{\rm c}/L_{\rm d}$). The inner disc radii were calculated from the normalizations of the irradiated disc models reported in Soria et al. (2012) ($N_{\rm disc} = 40.6^{+91.7}_{-13.5}$), Table 2 and the best-fitting normalization of $N_{\rm disc} = 60^{+90}_{-40}$ obtained for the young stellar population solution reported in Farrell et al. (2012) using the relationship $N_{\rm disc} = [(r_{\rm in}/\mathrm{km})/(D/10\,\mathrm{kpc})]^2 \cos i$ and an assumed distance of $D = 95$ Mpc. For disc angle of inclinations ranging from face-on ($i = 0°$) to $i = 75°$ (constrained via the absence of eclipses in the HLX-1 *Swift* XRT light curve), the inner disc radii agree between Farrell et al. (2012), Soria et al. (2012) and this work (see Table 3) with values around 10^5 km, indicative of a black hole mass of $\sim 10^4\,M_\odot$.

In contrast, the fraction of flux thermalized in the outer disc ($f_{\rm out}$) differed significantly from the values obtained from fitting the *HST*+S1 data alone by Farrell et al. (2012) and the value assumed by Soria et al. (2012), although still well within the physically

[3] See http://www.maraston.eu

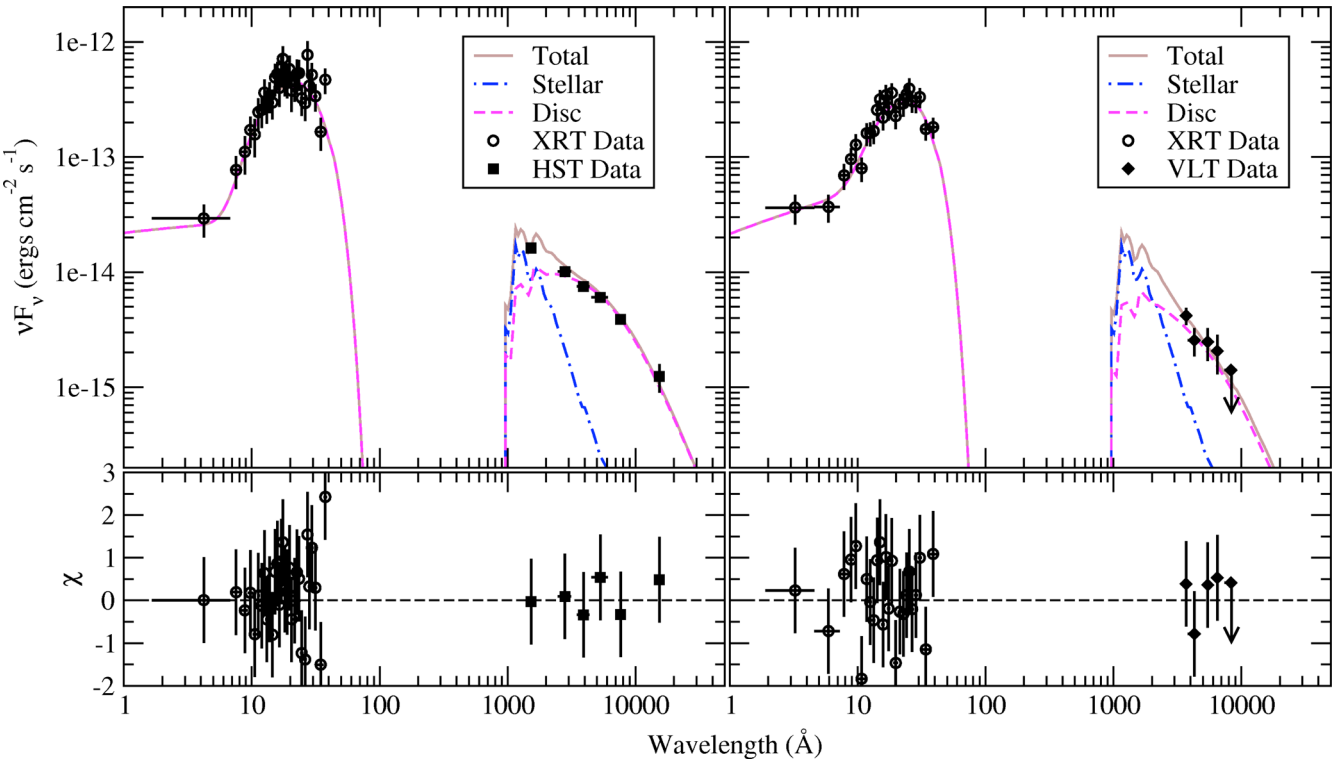

Figure 1. Best-fitting broad-band SED model of HLX-1 constructed using the *Swift* XRT, *HST* and VLT data fitted with the stellar population and irradiated disc models. Left: the *HST*+S1 data. Right: the VLT+S2 data. The bottom panels show the fit residuals.

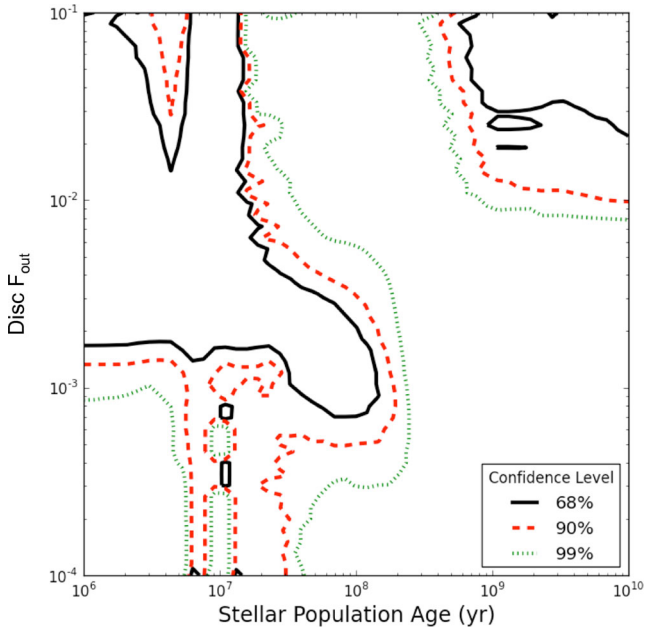

Figure 2. χ^2 contour plot of the stellar population age (using the Maraston 2005 theoretical stellar population model) versus the fraction of flux thermalized in the outer disc (f_{out}) for the fit to the *HST*+S1 data (the fit parameters are those listed in Farrell et al. 2012).

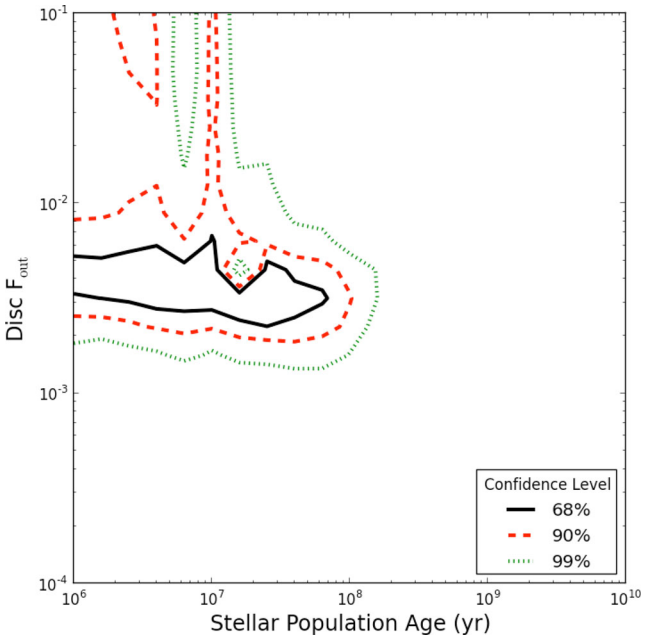

Figure 3. χ^2 contour plot of the stellar population age versus the fraction of flux thermalized in the outer disc (f_{out}) for the simultaneous fit to the *HST*+S1 and VLT+S2 data. The contours shown are for the irradiated disc model fitted to the *HST* data.

plausible range. The ratio of the outer to inner disc radii, $\log(r_{out}/r_{in})$, obtained from the combined fit to the *HST*+S1 and VLT+S2 data was also larger than the values obtained by Farrell et al. (2012) and assumed by Soria et al. (2012), indicating a larger outer disc radius of $\sim 10^{8-9}$ km. Such a large outer disc radius is impossible to reconcile with the rise and decay time-scales observed in the *Swift* XRT light curve, which suggest outer disc radii of $\sim 10^7$ km (assuming a viscosity parameter of $\alpha \sim 0.1$–1.0, similar to that observed in Galactic black holes; Lasota et al. 2011; Soria et al. 2012).

Table 3. Comparison of inner and outer accretion disc size constraints between the results obtained by Farrell et al. (2012), Soria et al. (2012) and the SED fits reported in this paper.

Data	$r_{\rm in}$ (10^5 km)	$r_{\rm out}$ (10^8 km)
$i = 0^\circ$		
HST+S1 (Farrell et al. 2012)	0.4–1.2	1.1–2.9
HST+S1 (this work)	0.4 – 0.7	2.7–16.9
VLT+S2 (Soria et al. 2012)	0.5–1.1	1.5–3.1
VLT+S2 (this work)	0.5–1.0	3.3–23.9
$i = 75^\circ$		
HST+S1 (Farrell et al. 2012)	0.8–2.3	2.1–5.7
HST+S1 (this work)	0.8–1.3	5.3–33.2
VLT+S2 (Soria et al. 2012)	1.0–2.1	2.9–6.0
VLT+S2 (this work)	1.0–1.9	6.5–46.9

However, we caution that these results are dependent upon the observed variability in the optical bands between the *HST* and VLT observations being real, yet the different background subtraction methods applied to the two optical data sets could produce apparent variability. In the next section, we present an analysis of optical monitoring data obtained with the Gemini-South telescope following the third X-ray outburst, in order to test whether the observed variability between the *HST* and VLT observations is real (assuming that the optical flux and spectrum variations are identical from outburst to outburst).

2.2 Gemini GMOS observations

We observed ESO 243−49 with Gemini Multi-Object Spectrograph-South (GMOS-S) at Gemini-South (Programme ID: GS-2011B-Q-31; see Hook et al. 2004, for an instrument description) using the r' filter (r_G0326, which covers the redshifted Hα emission line at ∼6720 Å) between 2011 August 31 and and October 6 (see Table 4). The observations were performed in photometric weather conditions, in order to detect a faint point source on top of the galaxy emission, and were triggered during the month after the 2011 X-ray outburst of HLX-1. The detector pixel scale is 0.146 arcsec per pixel and we used a nine-point dither pattern repeated twice.

We used the THELI pipeline[4] (Erben et al. 2005) to process the images (using bias and twilight flat images), align the images on the USNO-B1 catalogue, and stack the dithered exposures. All images were then cropped to have a similar size and pixel scale. We selected seven isolated point-like stars in the field and estimated the encircled energy at different extraction radii (2 to 25 pixels). The sky was estimated in an annulus (25 to 27 pixels) and subtracted. From those stars, we also estimated the relative scale between the different exposures. The relative error for the scaling was 6 per cent in the r band.

We extracted the flux from the optical counterpart to HLX-1. We subtracted the extended emission of the galaxy locally using a thin plate spline method as implemented with the IDL procedure GRID_TPS (Barrodale et al. 1993). This function interpolates a set of values over a regular two-dimensional grid, from irregularly sampled data values, e.g. excluding a circular region of radius 5–7 pixels around the source in an image stamp. We then performed aperture photometry (radii of 4 pixels, encircling 50 to 70 per cent of the total energy), and corrected for losses as estimated from the encircle energy of reference stars. The extracted fluxes were then normalized to the mean of all four r'-band values. The errors include the error on the flux measurement (quadratic sum of the scatter in background values, the random photon noise, and the uncertainty in mean sky brightness) and the uncertainties from scaling and aperture corrections. The values are reported in Table 4 and in Fig. 4 (bottom panel). The relative errors are thus about 30–40 per cent, due to the fact that the source is faint and buried in the galaxy emission. An absolute measurement would include additional uncertainties, which is why we chose to use data from one instrument only and focused on relative errors in this work.

It is, however, possible to get a rough estimate of the magnitude. We used our seven reference stars and their magnitudes reported in the GSC 2.3 catalogue for the R^F band (Fmag in the catalogue). The conversion from R^F to r magnitudes is not colour dependent for point sources, so we can apply an additive correction of +0.4 mag to the Fmag values to get r'-band magnitudes (see e.g. Drimmel et al. 2004). We combined all four r'-band images and found a zero-point of 28.33 from our reference stars, with a 1σ error of 0.2. This is consistent with the zero-point given on the Gemini webpages[5] for GMOS-S (28.3–28.4). We applied this zero-point to the extracted flux of the target and combined the errors to estimate an average r'-band AB magnitude of 24.12 ± 0.3 over the 4 r'-band images. Assuming no colour dependence (and in fact the colour term for the HLX-1 counterpart is lower than the errors), this converts to a Vega R-band magnitude of 23.9 ± 0.3, consistent with the value at the end of 2009 August (23.8 ± 0.25; Soria et al. 2010) and in 2010 September (Farrell et al. 2012), but brighter than the magnitude in 2010 November, three months after the outburst (24.7 ± 0.4; Soria et al. 2012).

We show in Fig. 4 the X-ray count rate from our follow-up programme with the *Swift* XRT over a similar period of time. We used the web based interface[6] (Evans et al. 2009) to extract the count rate for each observation, and with a binning of 100 counts per bin. The count rates were then normalized to the mean count rate over MJD 557 92 and 558 52 (the area not shaded in Fig. 4, top panel). We fitted the X-ray light curve with an exponential decay, and overplot the same function over the r'-band light curve (Fig. 4, bottom panel). It is clear from Fig. 4 that the r'-band fluxes are consistent with both a constant and an exponential decay.

3 DISCUSSION AND CONCLUSIONS

3.1 The combined SED fitting

In this paper, we have presented a combined analysis of *HST*, VLT and *Swift* observations of the IMBH HLX-1 taken ∼2 months apart during the decay following the outburst in 2010. By fitting the VLT+S2 data simultaneously we confirm that these data are entirely consistent with an irradiated disc model without the need for an additional stellar component. However, the *HST*+S1 data are not consistent with such a model, with a clear UV excess present in the SED (as previously reported in Farrell et al. 2012). When fitted

[4] http://www.astro.uni-bonn.de/∼theli/

[5] http://www.gemini.edu/sciops/instruments/performance-monitoring/data-products/gmos-n-and-s/photometric-zero-points

[6] http://www.swift.ac.uk/user_objects/

Table 4. Gemini GMOS r'-band filter observations of HLX-1.

Night	MJD	Date	Exp. time (s)	Airmass	Seeing	Relative flux
1	55804.267	2011-08-31T06:25:17.1	4832.82	1.05	0.83	0.91 ± 0.37
2	55810.182	2011-09-06T04:22:20.6	4832.82	1.13	0.67	1.07 ± 0.37
3	55828.205	2011-09-24T04:55:49.4	4832.82	1.05	0.45	0.96 ± 0.26
4	55840.100	2011-10-06T02:23:37.5	4027.35	1.14	0.66	1.06 ± 0.31

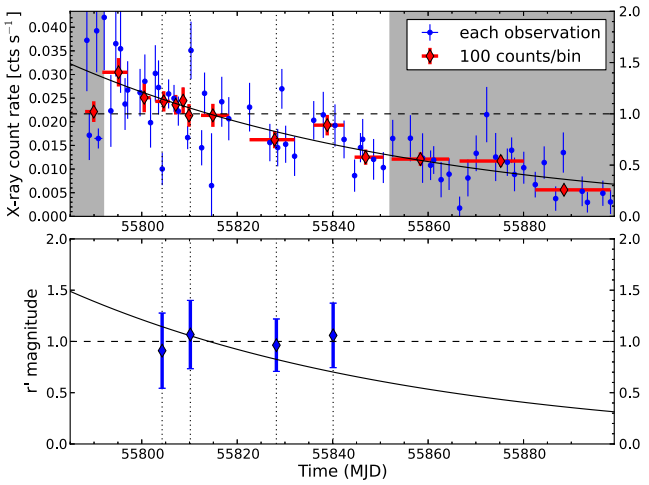

Figure 4. *Swift* XRT (top panel) and Gemini r'-band (bottom panel) light curves of HLX-1. The right-hand axis in the top panel shows the normalized flux. The dashed lines indicate the mean X-ray (top) and optical (bottom) fluxes over the period not shaded in the top panel. The black lines indicate the exponential fit to the binned X-ray light curve.

without the far-UV data point, the *HST*+S1 SED is well described by the irradiated disc model, highlighting the importance of UV data for disentangling the disc and stellar population contributions.

In an attempt to break the degeneracies posed by these two model components, we fitted the *HST*+S1 and VLT+S2 data simultaneously with a model representing emission from an irradiated disc plus a stellar population. The parameters of the disc components derived from the SED fitting are entirely physical, obtaining inner disc temperatures of 0.17–0.20 keV (consistent with previous results and with emission from a geometrically thin, optically thick accretion disc), reprocessing fractions of 0.08–0.37 per cent, inner disc radii of $\sim 10^{4-5}$ km, and an outer disc radius of $\sim 10^{8-9}$ km, all consistent with an accretion disc around a $\sim 10^4$ $M_\odot$ black hole. The presence of reprocessing in the outer accretion disc would definitively rule out beaming as the cause of the high X-ray luminosity of HLX-1, indicating that the emission must be isotropic and thus strongly supportive of the presence of an IMBH.

We found that the simultaneous SED fitting of both epochs of data is inconsistent with the old stellar population solutions derived by Farrell et al. (2012) and Soria et al. (2012), suggesting instead a stellar age of ∼20 Myr. The best-fitting solution indicates a higher contribution by an irradiated accretion disc than found by Farrell et al. (2012), resulting in a lower stellar luminosity and thus a lower mass for the stellar cluster of $\sim 10^5$ $M_\odot$. However, the data do not exclude the presence – in addition to the population of young stars that dominate the stellar light – of a lower luminosity population of older (∼10 Gyr) stars with a total stellar mass up to $\sim 10^6$ $M_\odot$. It is well known that composite populations containing a large gap in stellar ages are difficult to disentangle, because the energetic emission of stellar populations with ages smaller than ∼100 Myr is orders of magnitudes larger than those from older stars, and dominate the spectrum at all optical and near-IR wavelengths (see e.g. Maraston et al. 2010, fig. 12). These results continue to support the scenario whereby HLX-1 is the remnant of a dwarf galaxy that has been accreted and stripped of most of its mass through a merger event with ESO 243−49. In this framework, a higher total mass of the stellar cluster than that derived for the dominant population of young stars (thus implying that an older population of low luminosity stars may dominate the mass) is likely required in order to explain how HLX-1 managed to retain the gas necessary for the recent burst of star formation.

3.2 Constraints on the nature of the donor star

Having a young stellar population opens up the possibility of having a supergiant or Wolf–Rayet donor star. In both cases, the high mass-loss rates could be sufficient to power HLX-1. Additionally, there is good evidence, both theoretical (see Frank, King & Raine 2002) and observational (see e.g. Smith, Heindl & Swank 2002) that the outer accretion disc radii in systems fed by fast winds may be smaller than those fed by Roche lobe overflow. In the event that the system is wind fed, the possibility then remains that the fast rise time-scales of the outbursts might be explained without requiring the extremely large eccentricities and the small radii invoked in Soria (2013). This scenario will be investigated further in a future paper (Miller et al., in preparation).

3.3 The optical variability

The apparent change in optical brightness between different epochs strongly implies that the irradiated disc provides the dominant contribution to the optical continuum (not including the far-UV band). Specifically, $R \approx 23.8 \pm 0.1$ mag in the *HST* observations (obtained by interpolating the optical continuum between the V and I bands) and $R \approx 23.9 \pm 0.3$ mag in the Gemini data (both observed about a month after the X-ray outburst), but $R \approx 24.7 \pm 0.4$ mag in the VLT images (three months after outburst). However, it is possible that this optical variability may be artificial, a result of the different background subtraction methods applied. For the *HST* data, the background light from ESO 243−49 was simply subtracted from a nearby region using standard aperture photometry, as the superior angular resolution of the *HST* allows us to resolve out the background contribution from the host galaxy. The VLT data of ESO 243−49 were modelled by fitting the local galaxy background around HLX-1 with a thin plate spline model (similar to the approach we adopted for the Gemini GMOS data, with similar magnitudes derived) and then subtracted prior to measuring the photometry. The errors were bootstrapped from this fitting procedure and thus include the effects of uncertainty in the local background. This is crucial, since the photometric errors are dominated by the local background estimate and any background estimation error would introduce spurious variability when comparing to the *HST* data.

Gemini observations in the r'-band covering part of the decay of the third X-ray outburst in 2011 show no evidence for any significant variability in optical bands but do not rule out variability < 50 per cent. Nonetheless, an exponential decay similar to that observed in X-rays is not ruled out by the Gemini data. We also compared each r'-band observation with the closest X-ray observation in time (1, 2, 5 and 7 h difference for nights 1 to 4, respectively). No correlation was observed, though we note that this could be due to the low number of counts detected in each *Swift* XRT observation. In addition, fluctuations in the binned X-ray light curve are not correlated with the r'-band light curve.

We stress that the Gemini data do not rule out the presence of variability, but instead indicate that it is important to compare optical data taken with the same telescope and instrument setup and using the same background subtraction method in order to confirm the variability and thus constrain the parameters of the SED model components. Further observations with the *HST* or longer term monitoring with ground based 8 m class telescopes at different X-ray luminosities are thus necessary in order to definitively break the degeneracies in the SED fitting and thus confirm the age and mass of the stellar cluster, as well as the fraction of reprocessing in the accretion disc.

ACKNOWLEDGEMENTS

We thank the anonymous referee for their comments that improved this paper as well as Tal Alexander, Cole Miller and Chris Done for useful discussions. SAF is the recipient of an Australian Research Council Postdoctoral Fellowship, funded by grant DP110102889. MS acknowledges support from the Centre National dEtudes Spatiales (CNES) and from programme number HST-GO-12256, which was provided by NASA through a grant from the Space Telescope Science Institute, which is operated by the Association of Universities for Research in Astronomy, Inc., under NASA contract NAS5-26555. JCG acknowledges support from the Avadh Bhatia Fellowship and Alberta Ingenuity. Based on observations made with the NASA/ESA *HST* associated with programme 12256. Based on observations made with ESO Telescopes at the Paranal Observatory under programme ID 088.D-0974(B). Based on observations obtained at the Gemini Observatory, which is operated by the Association of Universities for Research in Astronomy, Inc., under a cooperative agreement with the NSF on behalf of the Gemini partnership: the National Science Foundation (United States), the National Research Council (Canada), CONICYT (Chile), the Australian Research Council (Australia), Ministério da Ciência, Tecnologia e Inovação (Brazil) and Ministerio de Ciencia, Tecnología e Innovación Productiva (Argentina). We thank the *Swift* team for granting us Target of Opportunity observations in support of this programme.

REFERENCES

Abbott B. P. et al., 2009, Phys. Rev. D, 80, 062001
Arnaud K. A., 1996, in Jacoby G. H., Barnes J., eds, ASP Conf. Ser. Vol. 101, Astronomical Data Analysis Software and Systems V. Astron. Soc. Pac., San Francisco, p. 17
Barrodale I., Skea D., Berkley M., Kuwahara R., Poeckert R., 1993, Pattern Recognit., 26, 375
Begelman M. C., 2002, ApJ, 568, L97
Belczynski K., Bulik T., Fryer C. L., Ruiter A., Valsecchi F., Vink J. S., Hurley J. R., 2010, ApJ, 714, 1217
Cardelli J. A., Clayton G. C., Mathis J. S., 1989, ApJ, 345, 245
Davis S. W., Narayan R., Zhu Y., Barret D., Farrell S. A., Godet O., Servillat M., Webb N. A., 2011, ApJ, 734, 111
Drimmel R., Smart R., Spagna A., Bucciarelli B., Lattanzi M. G., McLean B., 2004, in Clemens D., Shah R., Brainerd T., eds, ASP Conf. Ser. Vol. 317, Milky Way Surveys: The Structure and Evolution of our Galaxy. Astron. Soc. Pac., San Francisco, p. 193
Erben T. et al., 2005, Astron. Nachr., 326, 432
Evans P. A. et al., 2009, MNRAS, 397, 1177
Farrell S. A., Webb N. A., Barret D., Godet O., Rodrigues J. M., 2009, Nat, 460, 73
Farrell S. A. et al., 2011, Astron. Nachr., 332, 392
Farrell S. A. et al., 2012, ApJ, 747, L13
Fornasa M., Bertone G., 2008, Int. J. Mod. Phys. D, 17, 1125
Frank J., King A., Raine D. J., 2002, Accretion Power in Astrophysics. Cambridge Univ. Press, Cambridge
Freeland M., Kuncic Z., Soria R., Bicknell G. V., 2006, MNRAS, 372, 630
Gierliński M., Done C., Page K., 2008, MNRAS, 388, 753
Gierliński M., Done C., Page K., 2009, MNRAS, 392, 1106
Godet O., Barret D., Webb N. A., Farrell S. A., Gehrels N., 2009, ApJ, 705, L109
Godet O. et al., 2012a, ApJ, 752, 34
Godet O., Webb N., Barret D., Farrell S., Gerhels N., Servillat M., 2012b, Astron. Telegram, 4327, 1
Hook I. M., Jørgensen I., Allington-Smith J. R., Davies R. L., Metcalfe N., Murowinski R. G., Crampton D., 2004, PASP, 116, 425
Hopkins P. F., Bundy K., Hernquist L., Wuyts S., Cox T. J., 2010, MNRAS, 401, 1099
Kalberla P. M. W., Burton W. B., Hartmann D., Arnal E. M., Bajaja E., Morras R., Pöppel W. G. L., 2005, A&A, 440, 775
King A. R., 2008, MNRAS, 385, L113
King A. R., Ritter H., 1998, MNRAS, 293, L42
Lasota J.-P., Alexander T., Dubus G., Barret D., Farrell S. A., Gehrels N., Godet O., Webb N. A., 2011, ApJ, 735, 89
Lodders K., 2003, ApJ, 591, 1220
Maraston C., 2005, MNRAS, 362, 799
Maraston C., Pforr J., Renzini A., Daddi E., Dickinson M., Cimatti A., Tonini C., 2010, MNRAS, 407, 830
Ricotti M., Ostriker J. P., 2004, MNRAS, 352, 547
Schlegel D. J., Finkbeiner D. P., Davis M., 1998, ApJ, 500, 525
Servillat M., Farrell S. A., Lin D., Godet O., Barret D., Webb N. A., 2011, ApJ, 743, 6
Shakura N. I., Sunyaev R. A., 1973, A&A, 24, 337
Smith D. M., Heindl W. A., Swank J. H., 2002, ApJ, 578, L129
Soria R., 2013, MNRAS, 428, 1944
Soria R., Hau G. K. T., Graham A. W., Kong A. K. H., Kuin N. P. M., Li I.-H., Liu J.-F., Wu K., 2010, MNRAS, 405, 870
Soria R., Hakala P. J., Hau G. K. T., Gladstone J. C., Kong A. K. H., 2012, MNRAS, 420, 3599
Soria R., Hau G. K. T., Pakull M. W., 2013, ApJ, 768, L22
Volonteri M., 2010, A&AR, 18, 279
Webb N. A., Barret D., Godet O., Servillat M., Farrell S. A., Oates S. R., 2010, ApJ, 712, L107
Webb N. A. et al., 2012, Sci, 337, 554
Wiersema K., Farrell S. A., Webb N. A., Servillat M., Maccarone T. J., Barret D., Godet O., 2010, ApJ, 721, L102

This paper has been typeset from a TEX/LATEX file prepared by the author.